

# Six-Axis Nanopositioning Device With Precision Magnetic Levitation Technology

Shobhit Verma, Won-jong Kim, *Senior Member, IEEE*, and Jie Gu

**Abstract**—In this paper, we present the design, control, and testing of a 6 degrees-of-freedom magnetically-levitated system with nanometer-precision positioning capability and several-hundred-micrometer travel range. This system levitates a triangular single-moving-part platen, and produces the six-axis motion with six single-axis linear actuators. One of the prominent advantages of this magnetic levitation (maglev) system is that there is no physical contact between the moving part and the stator, which eliminates friction, wear, backlash, and hysteresis. As compared to other traditional devices, the present system is very compact with the minimum number of actuators for six-axis motion generation. The maglev device presented herein shows the position resolution better than 5 nm with 2-nm rms position noise, and is capable of a velocity of 0.5 m/s and an acceleration of 30 m/s<sup>2</sup>. The nominal power consumption is only 15 mW by each horizontal actuator, and 320 mW by each vertical actuator. The actuators are sized to be able to orient and position a maximum payload of 1 kg. The key application of this maglev device is the manipulation at nanoscale for microassemblies and manufacture of their parts. Other potential applications are stereolithography, vibration-free delicate instrumentation, and microscale rapid prototyping.

**Index Terms**—Magnetic levitation (maglev) system, nanomanipulation, precision positioning, 6-degrees-of-freedom (6-DOF) motion, real-time digital control.

## I. INTRODUCTION

IN THE modern era of nanosystems, the precise manufacture of nanoparts is a very crucial task [1], [2]. An important factor that limits the manufacturing precision is the manipulation of the objects at nanoscale. The application of nanotechnology and high-precision manufacturing techniques will enable accurate manipulation and fabrication of nanostructures. In atomic-scale material handling, characterization, and manipulation, the objects under particular operations must be positioned and oriented accurately in all 6 degrees-of-freedom (DOF).

The development of the scanning tunneling microscope (STM) and the atomic force microscope (AFM) initiated atomic-level profiling and characterization [3], [4]. Although, their primary application was topographical imaging, these instruments became the prime tools for nanomanipulation.

Manuscript received April 25, 2003; revised July 29, 2003. This work was supported by the National Science Foundation under Grant CMS-0116642.

S. Verma is with the Department of Mechanical Engineering, Texas A&M University, College Station, TX 77840 USA (e-mail: shobhit@tamu.edu).

W. Kim is with the Department of Mechanical Engineering, Texas A&M University, College Station, TX 77843-3123 USA (e-mail: wjkim@mengr.tamu.edu).

J. Gu was with the Mechanical Engineering Department, Texas A&M University, College Station, TX 77840 USA. He is now with the Department of Electrical Engineering, University of Minnesota, Minneapolis, MN 55455 USA (e-mail: gujie0216@hotmail.com).

Digital Object Identifier 10.1109/TMECH.2004.828648

Notable shortcomings of such instruments are limited number of DOFs and small travel ranges; they are capable of limited manipulation in the  $x$ - $y$  plane with a travel range of 100  $\mu$ m and very small translation (a few micrometers) in the vertical direction with little rotational capability. Most of the actuators in these instruments are made of lead-zirconium-titanate (PZT) ceramics, which have downsides such as high-application voltage and nonlinearity.

A nanomanipulator system, which could interface with STMs, was developed by Taylor [5]. A 6-DOF magnetic levitation (maglev) positioner with air-core solenoids and permanent magnets was designed by Jung and Beak [6]. Sun *et al.* fabricated a dual-axis electrostatic microactuation system, which is capable of 0.01- $\mu$ m resolution in 5- $\mu$ m position change [7]. A high-stiffness linear piezoelectric motor with a resolution of 5 nm and output force of 200 N was demonstrated by Zhang [8]. Tan *et al.* applied a learning nonlinear proportional-integral-derivative (PID) controller for micropositioning of a linear piezoelectric motor [9]. Mori *et al.* demonstrated a high-bandwidth linear actuator consisting of an air-bearing and voice-coil motor, which is capable of 1-nm steps without overshoot or undershoot [10]. Dong *et al.* presented a 10-DOF nanorobotic manipulator actuated by PZT with a linear resolution of 30 nm and rotary resolution of 2 mrad [11]. An automated microrobot-based desktop station is applied for micro-assembly and handling of micro objects. These microrobots are capable of manipulation with 10-nm accuracy and several-mm/s speed [12]. A high-speed precision stage was made by use of a nonresonant-type ultrasonic motor that had a resolution of 0.69 nm [13].

The maglev technology can be a novel solution to nanopositioning thanks to its noncontact nature. It eliminates mechanical friction, stiction, backlash, and hysteresis that are detrimental to precise control. The application of the maglev technology has been proven to be very successful in precision motion control. Kim constructed a high-precision planar maglev stage with large planar motion capability which had 10-nm resolution and 100-Hz control bandwidth [14], [15]. Hollis *et al.* demonstrated a 6-DOF magnetically levitated fine motion wrist, which is a good example of multi-axes maglev systems [16]. A multi-DOF magnetic suspension stage with robust nonlinear control was demonstrated by Shan *et al.* [17]. Holmes *et al.* designed a maglev scanning stage that is capable of 0.6-nm three-sigma horizontal position noise [18]. Hajjaji and Ouladsine fabricated and demonstrated a real-time nonlinear control model for a maglev stage [19].

The maglev instrument presented in this paper is shown in Fig. 1. It can position and orient the mounted specimen in all

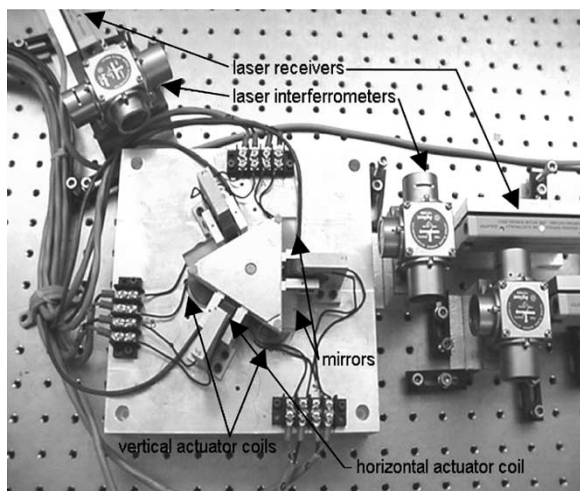


Fig. 1. Photograph of the six-axis maglev nanopositioning device.

6 DOFs with a position noise of 2 nm in translation and 300 nrad in rotation. It covers a large travel range of 300  $\mu\text{m}$  in translation and 3.5 mrad in rotation limited by the plane-mirror laser interferometry. The mechanical travel range is 52 mrad, but the laser beam goes out of its receiver if the mirror is rotated at an angle greater than 3.5 mrad. A preliminary design concept of the maglev device was presented in Kim and Maheshwari [20].

This compact maglev instrument has six single-axis actuators consisting of permanent magnets and current-carrying coils. The precision positioning is performed with the controlled coil currents. The system uses three laser interferometers and three capacitance gauges to sense the 6-DOF position of a single levitated part, namely the platen. The real-time control laws are implemented in a digital signal processor (DSP). A VME PC is used to give user commands and to monitor the real-time operation of the maglev system. A data acquisition board is being used to acquire the analog data from capacitance sensors and to give output to the power amplifiers.

This maglev device is in a very compact structure with extended travel and fine resolution in all 6 DOFs. Significant advantages in our concept over other existing maglev devices, especially Hollis' device include: 1) the moving part is completely physically isolated from the static part, and there is no cable connection; this fact prevents the transmission of nanoscale vibration from the environment; 2) the moving part carries only permanent magnets without iron core, which makes it light weight. Absence of iron eliminates eddy current, and the control loop can be closed at high bandwidth; 3) there is no  $I^2R$  loss in the moving platen, which avoids thermal distortion; and 4) the actuator is of air-core type and its design is very simple and easy to implement without the difficulty of complicated assembly and alignment problems.

In the following sections, we discuss the mechanical design, instrumentation structure, modeling, and control of this maglev nanopositioning system. Representative experimental results verify its nanopositioning capabilities.

## II. MECHANICAL STRUCTURE

Fig. 2 is an exploded view of the mechanical assembly and shows all key parts in detail. On the base plate 3, capacitance

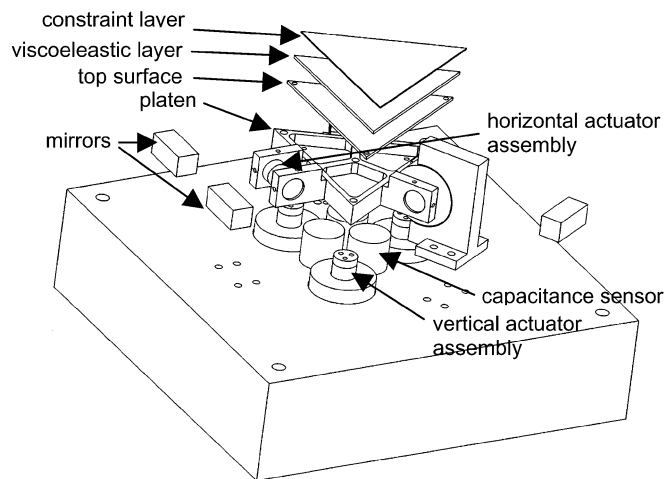


Fig. 2. Exploded view of the mechanical assembly.

sensors are mounted in the center. Just above them is a triangular single-moving part, the platen. This maglev system levitates the platen mass of 0.2126 kg. The core of this platen is made of pocket-milled single-piece aluminum to reduce its mass and to keep its natural frequency high to enhance system stiffness. A finite-element analysis shows the natural frequency of the platen at as high as 4.6 kHz. An aluminum top surface is fixed with four screws on the platen core. A viscoelastic damping layer, a stainless-steel constraint layer, and the top-surface are glued together with double-sided tapes. The purpose of this viscoelastic damping is to damp out the vibration and resonance of the platen to improve system stability.

The platen carries the magnet pieces in the six linear single-axis actuators numbered as in Fig. 3(a). For the design, analysis and testing of these single-axis magnetic actuators, refer to Kim and Maheshwari [20]. At its three corners are three vertical actuators ( $v_1$ ,  $v_2$ , and  $v_3$ ) that make it move in the three vertical DOFs, i.e.,  $z$  translation and rotations about the  $x$ - and  $y$ -axes ( $\psi$  and  $\theta$ ). In the middle of the three arms are three horizontal actuators ( $h_1$ ,  $h_2$ , and  $h_3$ ) that generate forces in the three horizontal DOFs, i.e.,  $x$ - and  $y$ -translations and rotation about the  $z$  axis ( $\phi$ ). The forces generated by the vertical actuators are shown as  $f_{v1}$ ,  $f_{v2}$ , and  $f_{v3}$ , and by the horizontal actuators as  $f_{h1}$ ,  $f_{h2}$ , and  $f_{h3}$ . The conceptual modal force generation of the maglev system is depicted in Fig. 3. Fig. 3(b)–(g) shows the directions of forces by individual single-axis actuators to generate the platen motion in any particular axis.

## III. INSTRUMENTATION STRUCTURE

Fig. 4 shows the schematic of the instrumentation structure of the maglev system. The Pentek 4284 board with a TMS320C40 DSP has been employed to perform the real-time digital control of the system. Sampling of position data, control variable calculation, and real-time control take place in the interrupt service routine (ISR) we wrote. A VME PC (VMIC 7751) and three laser-axis boards (Agilent 10 897B) are also on the VME chassis with the DSP board. The VME PC is used to download C codes to the DSP and to transfer the commands in real time via user

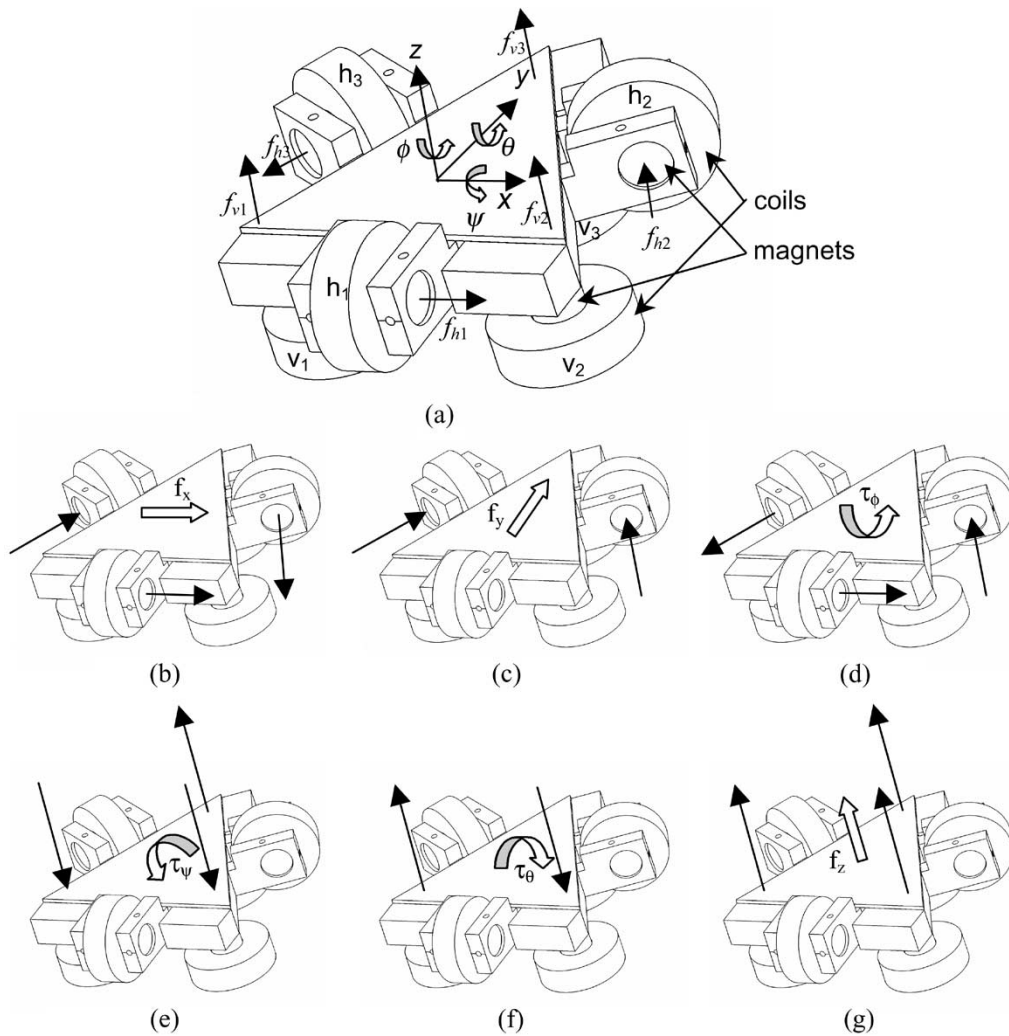


Fig. 3. (a) Convention of the coordinate axes and directions of forces by each single-axis actuator. The actuator force components  $f_{h1}$ ,  $f_{h2}$ , and  $f_{h3}$  are in the horizontal plane, and  $f_{v1}$ ,  $f_{v2}$ , and  $f_{v3}$  are in the vertical plane. (b)–(g) Directions of forces by each actuator to generate the six-axis modal forces/torques ( $f_x$ ,  $f_y$ ,  $f_z$ ,  $\tau_x$ ,  $\tau_y$ , and  $\tau_z$ ) acting on the platen center of mass. The transformation matrix between the modal forces/torques and the actuator forces is given in (4).

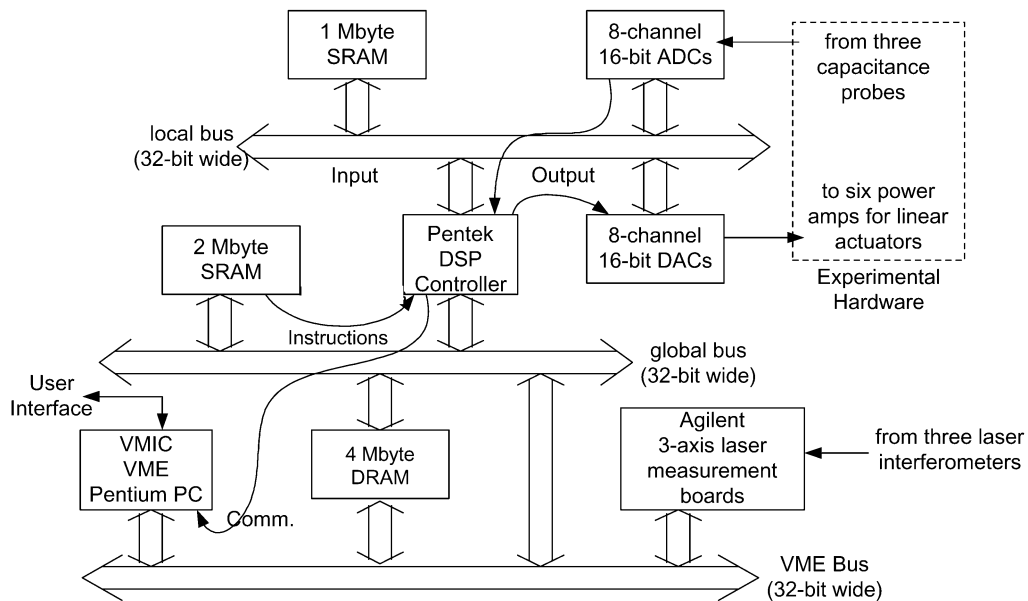


Fig. 4. Schematic diagram of the instrumentation structure.

interface during the maglev system operation. This communication between the DSP and the VME PC is established via a dual-port memory on the DSP board.

The three laser-axis boards give the position of the platen in the three horizontal DOFs at a resolution of 0.6 nm. The locations of these sensors are shown in Fig. 1. Digital 35-bit position and 24-bit velocity data are available directly from the laser-axis boards on the VMEbus with the refresh rate of 10-MHz. Three capacitance sensors (ADE 2810) are used for position feedback in the vertical axes, and are located just under the platen. These sensors are used with signal-conditioning units (ADE 3800) that pass the three vertical-axis position measurements to a data-acquisition board (Pentek 6102) through anti-aliasing filters. These anti-aliasing filters are a first-order *RC* low-pass filter with the corner frequency at 1 kHz. The data-acquisition board contains eight channels of 16-bit analog-to-digital converters (ADCs) and eight channels of 16-bit digital-to-analog converters (DACs) with the input/output range of  $\pm 5$  V.

The data-acquisition board communicates with the DSP via the MIXbus. The six channels of the DAC are used to give the control output to six transconductance amplifiers. Then, these amplifiers flow commanded currents through the actuator coils to generate the actuation forces. The main parts of the amplifiers are a differential amplifier, a feedback amplifier, and a power booster. The purpose of the differential amplifier is to remove common-mode noise from the DAC. The feedback amplifier is used to stabilize the current control loop. The power operational amplifier in the power booster is PA12A from Apex.

#### IV. DYNAMIC MODEL AND CONTROL STRUCTURE

The whole platen mass was measured 0.2126 kg by a precision balance. With the axis allocation in Fig. 3(a), the inertia matrix about the platen center of mass was calculated as follows:

$$[I] = \begin{bmatrix} I_{xx} & -I_{xy} & -I_{xz} \\ -I_{yx} & I_{yy} & -I_{yz} \\ -I_{zx} & -I_{zy} & I_{zz} \end{bmatrix} = \begin{bmatrix} 133 & -3.14 & 0 \\ -3.14 & 122 & 0 \\ 0 & 0 & 236 \end{bmatrix} 10^{-6} \text{ kg}\cdot\text{m}^2. \quad (1)$$

Since there is no physical contact in the platen with any other stationary parts, the platen can be modeled as a pure mass of 0.2126 kg. Thus, the system model for translation is

$$\frac{X(s)}{F(s)} = \frac{1}{0.2126s^2} \quad (2)$$

and for rotation

$$\frac{\Theta(s)}{T(s)} = \frac{1}{Is^2}. \quad (3)$$

The moment of inertia,  $I$ , in (3) can be  $I_{xx}$ ,  $I_{yy}$ , or  $I_{zz}$  depending on the axis. In the control system design, we neglect the products of inertia,  $I_{xy}$  and  $I_{yx}$  since they are less than 3% of any moment of inertia. Although, the force/torque acting on the magnet changes depending on its position inside the coil, this difference is not considered in the dynamic model because

the maximum amount of change calculated is less than 0.3% of the average force/torque for the whole 300- $\mu\text{m}$  travel range.

The modal forces/torques acting on the platen center of mass and the actuator forces are related by a force transformation matrix. We designed the maglev stage in such a way that the vertical DOFs ( $z, \psi, \theta$ ) and the horizontal DOFs ( $x, y, \phi$ ) are decoupled by placing the platen center of mass on the plane of the horizontal actuation. This collocation minimizes unmodeled erroneous coupling among the axes. This dynamic decoupling can be seen in the following force transformation matrix. The definition of force and torque components is shown in Fig. 3.

$$\begin{bmatrix} f_z \\ \tau_y \\ \tau_x \\ f_x \\ f_y \\ \tau_z \end{bmatrix} = \begin{bmatrix} 1 & 1 & 1 & 0 & 0 & 0 \\ l_{1x} & -l_{2x} & l_{3x} & 0 & 0 & 0 \\ -l_{1y} & -l_{2y} & l_{3y} & 0 & 0 & 0 \\ 0 & 0 & 0 & 1 & -\cos 60^\circ & -\cos 60^\circ \\ 0 & 0 & 0 & 0 & \cos 30^\circ & -\cos 30^\circ \\ 0 & 0 & 0 & l_{1z} & l_{2z} & l_{3z} \end{bmatrix} \times \begin{bmatrix} f_{v1} \\ f_{v2} \\ f_{v3} \\ f_{h1} \\ f_{h2} \\ f_{h3} \end{bmatrix}. \quad (4)$$

The various distance parameters are as follows:

- $l_{1x}$  from actuator  $v_1$  to the  $y$  axis along the  $x$  axis = 27.92 mm;
- $l_{1y}$  from actuator  $v_1$  to the  $x$  axis along the  $y$  axis = 15.16 mm;
- $l_{2x}$  from actuator  $v_2$  to the  $y$  axis along the  $x$  axis = 27.08 mm;
- $l_{2y}$  from actuator  $v_2$  to the  $x$  axis along the  $y$  axis = 15.16 mm;
- $l_{3x}$  from actuator  $v_3$  to the  $y$  axis along the  $x$  axis = 0.4152 mm;
- $l_{3y}$  from actuator  $v_3$  to the  $x$  axis along the  $y$  axis = 32.47 mm;
- $l_{1z}$  distance from actuator  $h_1$  to the  $z$  axis = 4.037 mm;
- $l_{2z}$  distance from actuator  $h_2$  to the  $z$  axis = 4072 mm;
- $l_{3z}$  distance from actuator  $h_3$  to the  $z$  axis = 4.143 mm.

Based on the dynamic model described earlier a lead-lag controller was designed with the damping ratio  $\zeta = 0.7$  and the phase margin  $\text{PM} = 50^\circ$  at the crossover frequency of 48 Hz

$$G_z(s) = \frac{K(s+130)(s+8)}{s(s+1130)} \quad (5)$$

where  $K$  is the gain of the controller. For  $x$ -,  $y$ -, and  $z$ -translation the value of  $K$  is  $6.7897 \times 10^4$  N/m. The values of  $K$  are 42.438, 9.052, and 75.329 N for  $\theta$ ,  $\psi$ , and  $\phi$ , respectively. We located a free pole at the origin to eliminate steady-state error. This continuous-time transfer function of the controller was converted to a discrete-time one by the zeroth-order-hold equivalence method with a 5-kHz sampling frequency, and implemented in the DSP.

#### V. EXPERIMENTAL RESULTS

The maglev device was tested extensively with the controller designed in the previous section. Fig. 5 shows various step responses with the step sizes of 10 nm, 1  $\mu\text{m}$ , 10  $\mu\text{m}$ , and 300  $\mu\text{m}$  in the  $x$  axis. Fig. 5(a) shows a very small step response of 10 nm with a position noise less than 2-nm rms. The position

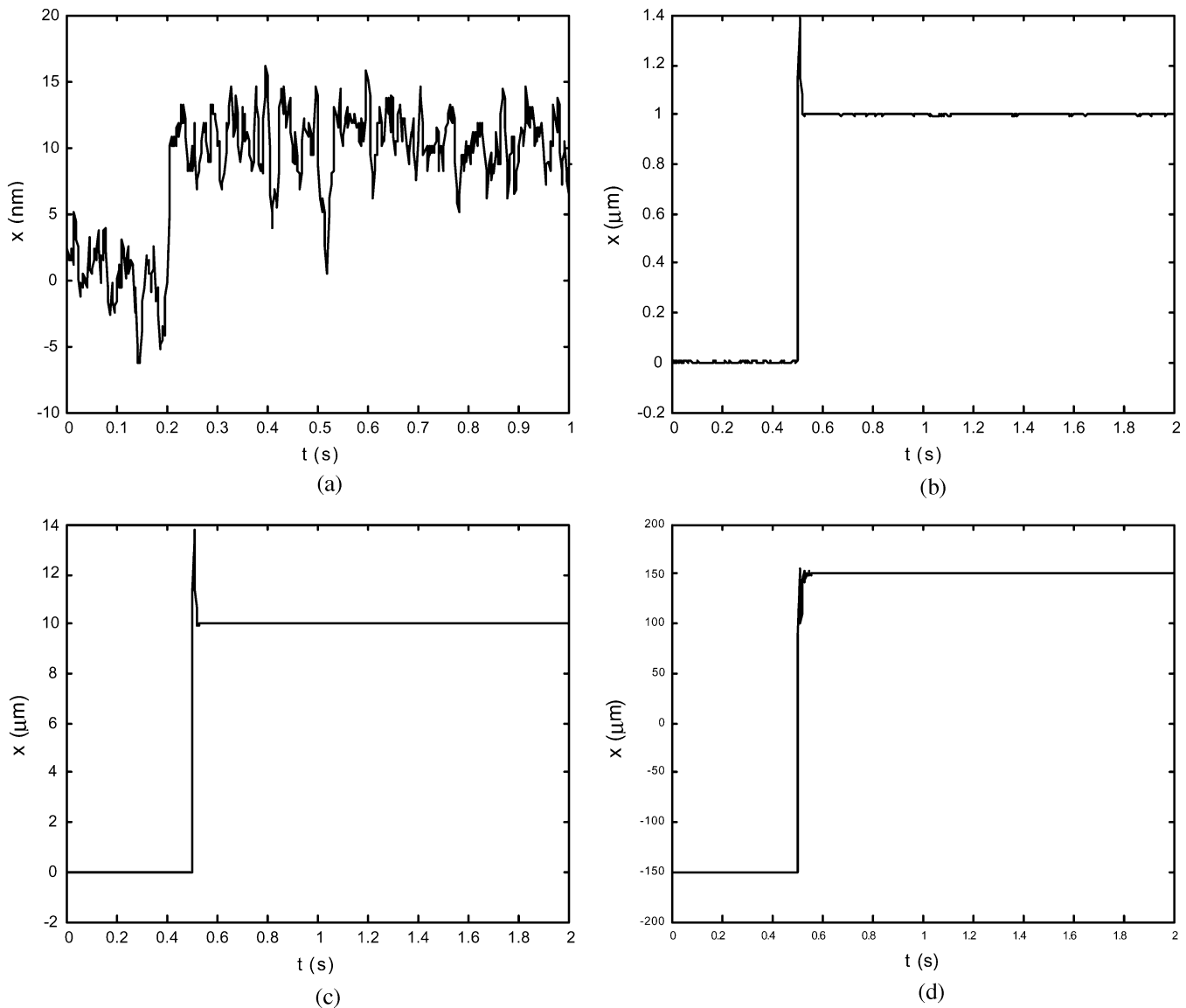


Fig. 5. Step responses in  $x$ : (a) 10 nm; (b) 1  $\mu\text{m}$ ; (c) 10  $\mu\text{m}$ ; and (d) 300  $\mu\text{m}$ .

resolution of the maglev stage is clearly better than 5 nm. In the medium-size steps of 1 and 10  $\mu\text{m}$  is no excessive oscillation in the responses, and the system settles in the commanded positions within 20 ms. A close inspection of the 300- $\mu\text{m}$  step response indicates that the system settled after some oscillations without overshoot. It is believed to be that one of the magnets attached to the platen hit the edge of the corresponding coil at the completion of the 300- $\mu\text{m}$  movement.

Coupling between horizontal and vertical motions existed due to the asymmetric location of the platen mass center and some mechanical assembly errors. This dynamic coupling between the vertical mode and the horizontal mode generated unwanted erroneous motions. The decoupling factors were calculated and incorporated in the force transformation matrix as the corresponding moment arms to reduce the cross talk. The results before and after the incorporation of these decoupling factors are shown in Fig. 6.

Fig. 7(a) shows the platen motion in  $x$  under 5-nm consecutive step commands with an interval of 0.4 s. The steps of 5-nm

can be clearly observed, which shows a 5-nm resolution. In Fig. 7(b) a response to a 280- $\mu\text{m}$  peak-to-peak saw-tooth input command is shown. The platen is able to traverse the whole 300- $\mu\text{m}$  travel range in 20 ms. The trajectory is not straight right after the direction reversal due to the abrupt change in acceleration. The maximum speed of this maglev stage is 0.5 m/s limited by the laser head specifications.

A 10-nm-radius circle traversed by the platen in the  $x$ - $y$  plane with a reference circle is shown in Fig. 8(a). The platen closely follows the circle with an average radius of 10.3 nm with a standard deviation of 2.5 nm. This test result demonstrates that the maglev device can track small trajectories and achieve position control at nanoscale precision.

Fig. 8(b) gives a three-dimensional (3-D) conical motion of a 40- $\mu\text{m}$  radius and a 50- $\mu\text{m}$  height generated by the maglev stage. This experimental result shows that the maglev stage can perform a complex 3-D positioning task precisely. Therefore we foresee an application of this maglev stage in 3-D microscale rapid prototyping.

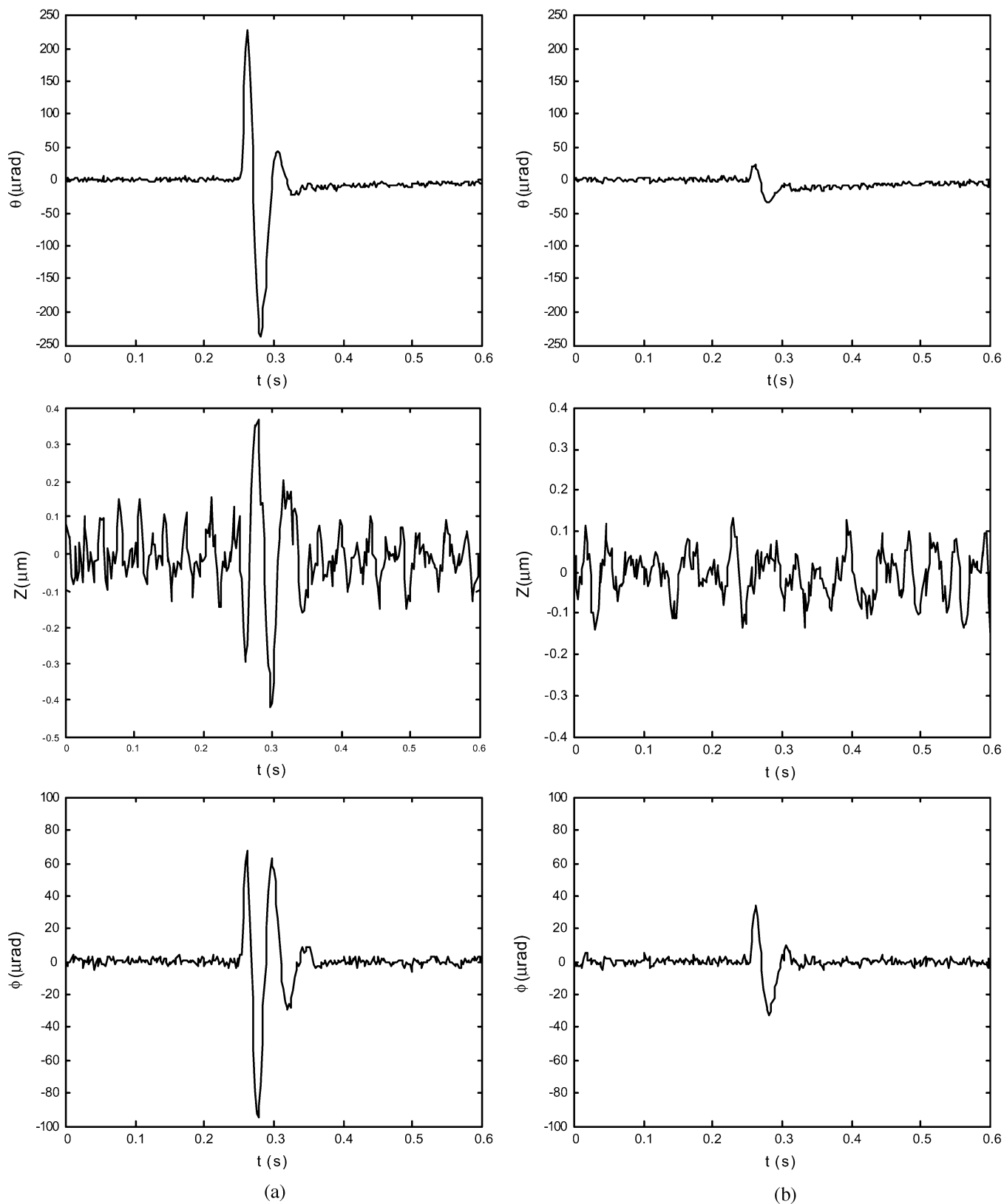


Fig. 6. Responses in other axes with a 50-μm step in  $x$ : (a) without and (b) with the incorporation of the decoupling factors.

### VI. CONCLUSION

In the near future, applications in nanotechnology will increase significantly due to the demands in the manufacture of nano-sized parts and assemblies. To enhance the quality of these

parts, accurate positioning and manipulation at nanoscale is necessary. These instruments should be able to generate motions in multiple DOFs, with a long travel range with nanoscale resolution. Thus precision instruments that can move and position the

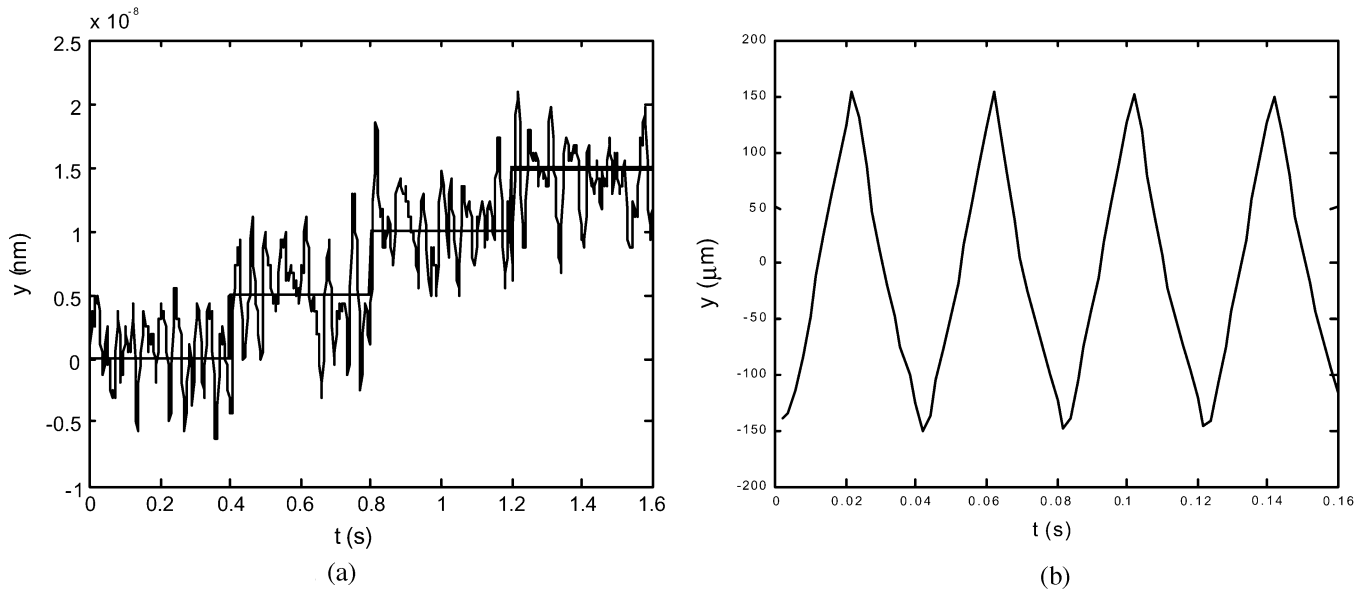


Fig. 7. (a) Platen motion in  $x$  under 5-nm consecutive step commands and the ideal line of path to follow, and (b) 280- $\mu\text{m}$  saw-tooth motion in  $y$ .

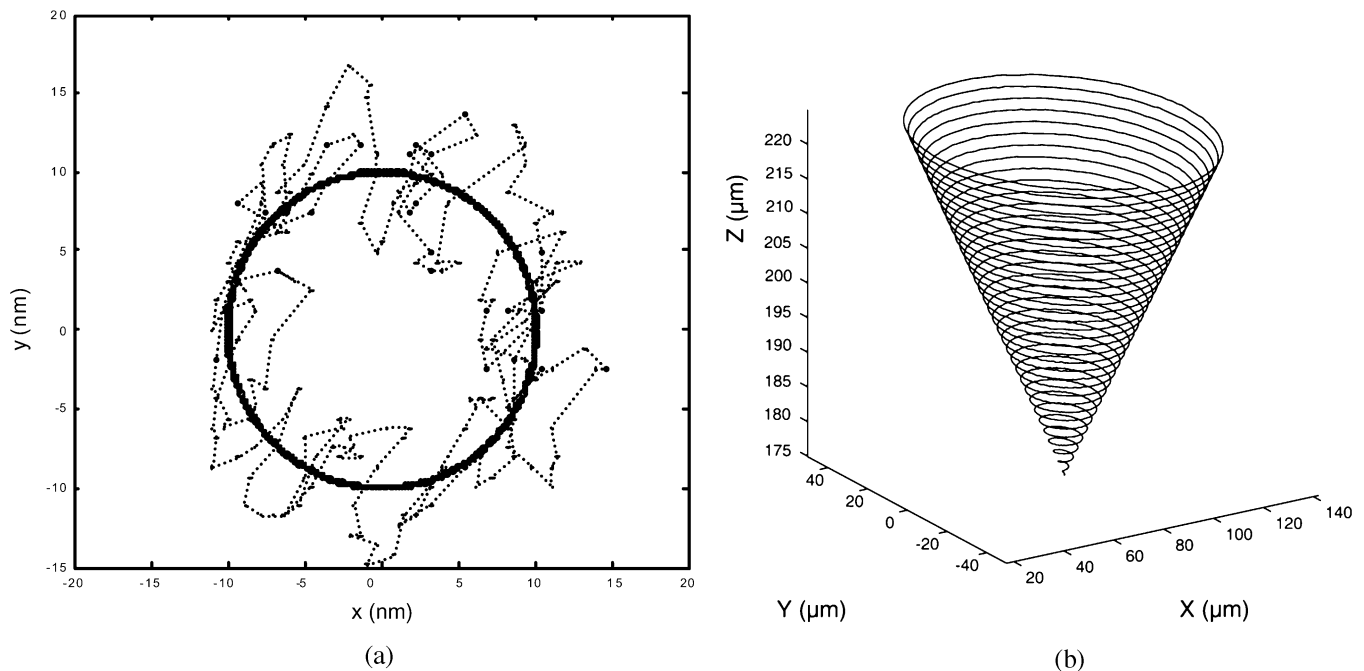


Fig. 8. (a) Circle with a 10 nm-radius traversed in the  $x$ - $y$  plane. (b) 3-D conical motion of a 40- $\mu\text{m}$  radius and a 50- $\mu\text{m}$  height generated by the maglev stage.

specimen in desired orientation with low vibration will play a crucial role in nanoscale manipulation.

In this paper, we presented a novel solution to this important problem based on precision magnetic levitation technology. The maglev system has no mechanical contact between the moving and stationary parts, which facilitates the maintenance of high position resolution. It also eliminates wear in the mechanical parts and increases their life spans, and does not require lubricants.

The compact maglev stage uses the minimum number of actuators required for 6-DOF motion generation. Prevailing precision positioning devices like STMs and AFMs are able to position in the travel range of 100  $\mu\text{m}$  in 3 DOFs. However, our

maglev device is capable of motion control in all 6 DOFs with the travel ranges of 300  $\mu\text{m}$  in the  $x$ -,  $y$ -, and  $z$ -translations and 3.5 mrad in the  $\theta$ -,  $\phi$ -, and  $\psi$ -rotations. The position resolution is better than 5 nm with position noise less than 2 nm rms. All the experiments were performed in a usual lab environment on a vibration-isolation optical table. This implies that in a controlled atmosphere and with a better ADC board we could have improved the noise performance. However, the correction of the ambient factors requires much more resources, and was beyond the scope of our project. We focused on the experimental demonstration of the fundamental working principles.

The dynamic performance of the maglev system was demonstrated with various experimental results, such as following a

saw-tooth trajectory of the whole travel range and consecutive steps of 5 nm. This system has the maximum speed capability of 0.5 m/s and the actuators are sized for 3-*g* acceleration (30 m/s<sup>2</sup>) in horizontal directions. The light-weight, compact design led to insignificant power consumption of 15 mW by each horizontal actuator and 320 mW by each vertical actuator in steady state.

The demonstration of small motions such as a 10-nm radius circle and a microscale conical motion verified the capability of this maglev device in extremely precise manipulation. Its capability to generate and control nanoscale motions in multiple axes can contribute significantly to the development of nanotechnology. This maglev device can be applied in various areas such as manipulation of nano-sized objects, and their manufacturing and assembly. Other potential applications will be stereolithography, vibration-free delicate instrumentation, and 3-D microscale rapid prototyping.

#### REFERENCES

- [1] "Nanoscale science, engineering and technology research directions," U.S. Department of Energy, CA, 2000.
- [2] *Nanotechnology: Shaping the World Atom by Atom*, The Interagency Working Group on Nanoscience, Engineering, and Technology (IWGN), Sept. 1999.
- [3] G. Binnig, H. Rohrer, C. H. Gerber, and E. Weibel, "Surface studies by scanning tunneling microscopy," *Phys. Rev. Lett.*, vol. 49, no. 1, pp. 57–61, July 5, 1982.
- [4] G. Binnig, C. F. Quate, and C. H. Gerber, "Atomic force microscope," *Phys. Rev. Lett.*, vol. 56, no. 9, pp. 930–933, Mar. 1986.
- [5] R. M. Taylor II, "The nanomanipulator: A virtual-reality interface to a scanning tunneling microscope," Ph.D. dissertation, Univ. North Carolina at Chapel Hill, NC, May 1994.
- [6] K. S. Jung and Y. S. Baek, "Study on a novel contact-free planar system using direct drive DC coils and permanent magnets," *IEEE/ASME Trans. Mechatron.*, vol. 2, pp. 35–43, Mar. 2002.
- [7] Y. Sun, D. Piyabongkarn, A. Sezen, B. J. Nelson, R. Rajamani, R. Schoch, and D. P. Potasek, "A novel dual-axis electrostatic microactuation system for macromanipulation," in *Proc. IEEE/RSJ Int. Conf. Intelligent Robots and Systems*, Oct. 2002, pp. 1796–1801.
- [8] B. Zhang and Z. Zhu, "Developing a linear piezomotor with nanometer resolution and high stiffness," *IEEE Trans. Mechatron.*, vol. 2, pp. 22–29, Mar. 1997.
- [9] K. K. Tan, T. H. Lee, and H. X. Zhou, "Micro-positioning of linear-piezoelectric motor based on a learning nonlinear PID controller," *IEEE Trans. Mechatron.*, vol. 6, pp. 428–436, Dec. 2001.
- [10] S. Mori, T. Hoshino, G. Obinata, and K. Ouchi, "Linear actuator with air bearing for highly precise tracking [HDD]," in *Dig. Asia-Pacific Magnetic Recording Conf.*, May 2002, pp. AP4-01–AP4-02.
- [11] L. Dong, F. Arai, and T. Fukuda, "3D nanorobotic manipulation of nano-order objects inside SEM," in *Proc. 2000 Int. Symp. Micromechanics and Human Science*, Mar. 2000, pp. 151–156.
- [12] S. Fatikow and U. Rembold, "An automated microrobot-based desktop station for micro assembly and handling of micro-objects," *Proc. Emerging Technologies and Factory Automation*, vol. 2, pp. 586–592, Nov. 1996.
- [13] Y. Egshira, K. Kosaka, S. Takada, T. Iwabuchi, T. Baba, S. Moriyama, T. Harada, K. Nagamoto, A. Nakada, H. Kubota, and T. Ohmi, "0.69 nm resolution ultrasonic motor for large stroke precision stage," in *Proc. IEEE Nanotechnology*, Oct. 2001, pp. 397–402.
- [14] W.-J. Kim, "High-precision planar magnetic levitation," Ph.D. dissertation, Massachusetts Inst. Technol., Cambridge, MA, June 1997.
- [15] W.-J. Kim and D. L. Trumper, "High-precision magnetic levitation stage for photolithography," *Precision Eng.*, vol. 22, no. 2, pp. 66–77, Apr. 1998.
- [16] R. L. Hollis, S. E. Salcudean, and A. P. Allan, "A six degree-of-freedom magnetically levitated variable compliance fine-motion wrist: Design modeling, and control," *IEEE Trans. Robot. Automat.*, vol. 7, pp. 320–332, June 1991.
- [17] X. Shan, S.-K. Kuo, J. Zhang, and C.-H. Menq, "Ultra precision motion control of a multiple degrees of freedom magnetic suspension stage," *IEEE/ASME Trans. Mechatron.*, vol. 7, pp. 67–78, Mar. 2002.
- [18] M. Holmes, R. Hocken, and D. L. Trumper, "The long-range scanning stage: A novel platform for scanned-probe microscopy," *Precision Eng.*, vol. 24, no. 3, pp. 191–209, July 2000.
- [19] E. Hajjaji and M. Ouladsine, "Modeling and nonlinear control of magnetic levitation systems," *IEEE Trans. Ind. Electron.*, vol. 48, pp. 831–838, Aug. 2001.
- [20] W.-J. Kim and H. Maheshwari, "High-precision control of a maglev linear actuator with nano-positioning capability," in *Proc. 2002 American Control Conf.*, May 2002, pp. 4279–4284.



**Shobhit Verma** was born in Aligarh, India, in 1979. He received the degree of B.Tech. in mechanical engineering and the M.Tech. degree in computer integrated manufacturing from Indian Institute of Technology, Bombay, India, in 2002. He is currently working toward the Ph.D. degree at Texas A&M University, College Station.

He is currently a Research Assistant at the Mechatronics Laboratory, Department of Mechanical Engineering, Texas A&M. His master's thesis work involved design and fabrication of an automatically-guided-vehicle system which had global vision based guidance and path planning. He worked in Crompton Greaves, India, as a summer trainee in during summer 2000. The work involved was toward the quality control and inventory management of the incoming parts and material. His research interests are magnetic levitation, precision positioning and nanofabrication.

During his undergraduate, he was the leading member of the winner team of the region XIII (outside North America) in the ASME student design contest and finalist in 2000. In 2001, his team represented the region XIII again and was ranked 5th in the international finals during ASME conference at New York. Mr. Verma is a student member of ASME.



**Won-jong Kim** (S'89–M'97–SM'03) received the B.S. (*summa cum laude*) and M.S. degrees in control and instrumentation engineering from Seoul National University, Seoul, Korea, in 1989 and 1991, respectively, and the Ph.D. degree in electrical engineering and computer science from Massachusetts Institute of Technology, Cambridge, in 1997.

In September 2000, he joined the Department of Mechanical Engineering, Texas A&M University, College Station, where he is currently an Assistant Professor. Following receipt of the Ph.D. degree, he was with SatCon Technology Corporation, Cambridge, MA, for three years. His teaching and research interests focus on analysis, design, and real-time control of mechatronic systems, and nanoscale engineering and technology.

Dr. Kim received the Grand Prize from the Korean Institute of Electrical Engineers' Student Paper Contest in 1988 and the Gold Prize for his doctoral work from Samsung Electronics' Humantech Thesis Prize in 1997. He was a semifinalist of the NIST's Advanced Technology Program 2000 Competition. The NASA granted him the Space Act Award in July 2002. He was appointed a Select Young Faculty Fellow by the Texas Engineering Experiment Station in September 2003. He is a member of ASME, ASPE, KSEA, Pi Tau Sigma, and Sigma Xi.



**Jie Gu** was born in China in 1979. He received the B.S. degree in precision instruments from Tsinghua University, Beijing, China, in 2001 and the M.S. degree in mechanical engineering from Texas A&M University, College Station, in 2003. He is currently working toward the Ph.D. degree in electrical engineering, at the University of Minnesota, Minneapolis.

His research interests are nanofabrication, MEMS, and precision engineering.